



Improve Waste Heat Recovery and Performance of Organic Rankine Cycle Analysis for Exhaust Gas from A Marine Diesel Engine Using Biofuel from Algae

Zalina Mat Nawi^{1,3,*}, Siti Kartom Kamarudin^{2,3}, Siti Rozaimah Sheikh Abdullah³

¹ Faculty of Ocean Engineering Technology & Informatics, Universiti Malaysia Terengganu, 21030 Kuala Terengganu, Terengganu, Malaysia

² Fuel Cell Institute, Universiti Kebangsaan Malaysia, 43600 UKM Bangi, Selangor, Malaysia

³ Department of Chemical Engineering, Faculty of Engineering and Built Environment, Universiti Kebangsaan Malaysia, 43600 UKM Bangi, Selangor, Malaysia

ARTICLE INFO

Article history:

Received 27 November 2022

Received in revised form 19 December 2022

Accepted 10 January 2023

Available online 1 February 2023

Keywords:

Organic Rankine cycle; Biofuel;

Microalgae

ABSTRACT

Marine diesel engines are commonly used as a propulsion system in ships. The waste heat generated from marine diesel engines is one of the key disadvantages of this system. This study aims to improve the recovery of waste heat generation. It presents the performance analysis of Organic Rankine Cycle (ORC) for exhaust gas in a marine diesel engine using different types of biofuels production methods from selected microalgae via mathematical modelling. The microalgae are from species of *Synechococcus PCC 7002*, *Nannochloropsis oculata* sp, *Chlorella protothecoides*, and *Dunaliella* sp. A marine engine with an exhaust gas of 9086.61 kg-h⁻¹ is taken as a case study. While the conventional diesel engine has a performance efficiency of 30-40% with a power output of 35-200K, this study has indicated that the marine diesel engine in the ORC via biofuel from algae shows higher performance at approximately 51% with a net power output of approximately 160kW obtained for each biofuel. Later, the thermal efficiency of the ORC system with exhaust gas from the marine diesel engine as waste heat recovery is improved to 61% with a net power output of approximately 353kW after the heat integration. Biodiesel presents the highest mass flow rate (1.12 kg-s⁻¹) compared to others. This study proved that biofuel from microalgae can achieve the highest performance in the ORC system with the lowest mass flow rate of biofuel compared to those in conventional fuel.

1. Introduction

The efficiency of diesel engines is only approximately 35%, while the remaining energy being released into the atmosphere. Even though improvements in diesel engine efficiency are still ongoing, a large amount of energy is still emitted to the surroundings with the exhaust gas [1-2]. Thimmanoor [3-5] states that, based on the heat balance of marine engines, the exhaust gas is the largest source of waste heat energy with a relatively higher temperature. The high source

* Corresponding author.

E-mail address: zalina@umt.edu.my

<https://doi.org/10.37934/araset.29.3.120>

temperature is beneficial due to its leading to a relatively larger difference between the evaporation and condensation temperatures of the working fluid.

The term 'waste heat recovery' is significantly related to improved energy utilization. In combination with engine development, the reuse of waste heat from diesel engines for useful work may increase system efficiency and decrease fuel consumption and production of acidic gas [6-8]. There are six important main factors that need to be taken into consideration, as they possibly disturb the possibility of waste heat recovery, namely, temperature, pressure, pressure drops, flow rate, allowable temperature, and chemical composition. The total availability of energy in waste heat sources can be determined by temperature, flow rate, specific heat, or the enthalpy of the waste heat stream [9-12].

Organic Rankine cycles (ORC) operate from low-temperature heat sources are commonly used for power generation. The available energy resources are solar energy, wind, biomass products, geothermal energy, surface seawater, and others, including waste heat from various thermal processes [13-17]. For temperature below 200°C, Isobutene is a common working fluid, while toluene is often used at higher source temperatures. Several studies have shown that pentane, propane, heptane, hexane, aromatics such as toluene and benzene, and refrigerants such as R113, R114, and R22 [18] are fluids that have been used for ORC applications.

As their oil production is far higher than that of terrestrial plants, biofuels from microalgae feedstock have been shown to be potential feedstock for future organic working fluids. Microalgae feedstock does not compete with food supplies and does not require high quality agricultural land; the supply is available continuously, it is able to grow under harsher condition, it is non-edible, and it shows highly genetically modifiable nature and fast growth rate when compared with conventional fuel [14-18]. In addition, the main advantages of using biofuels from microalgae as organic working fluids in an ORC system compared to a conventional fuel include the following: (i) it does not produce hazardous waste or pollution, (ii) it is carbon neutral, (iii) it produces highly biodegradable biofuels and less toxic, (iv) and it has a lower vapour pressure [19, 21, 23-26]. Some of microalgae and bacteria can act as self-propelled up swimming microorganisms and can be categorised as oxytaxis, gyrotaxis and gravitaxis [27].

However, very few studies regarding the production of biofuel from microalgae as working fluids in the ORC have been reported. Thus, this work studies the potential via the performance analysis of microalgae biofuel from selected species as the organic working fluid in the ORC system. This study presents the improved waste heat recovery and performance of ORC for exhaust gas from a marine diesel engine using biofuel from algae. The selected of marine diesel engine was a combined parameter of an inline six-cylinder turbocharged engine developed by Hudong Heavy Machinery Co. Ltd., [28] and a dual fuel low-temperature combustion engine [29]. This paper is consisting of four parts. The first part offers a general overview of the organic Rankine cycle and sets out the guidelines for this paper. The second part will describe the overall system design and show conceptual design through a description of each unit in the system. The third part will present the overall material balance and prediction of volume cultivation from microalgae culture. In the last part, the heat balance of the system and heat integration based on different biofuels will be presented. In the case study, the exhaust gas capacity was assumed to be $9086.61\text{kg}\cdot\text{h}^{-1}$ based on 996kW of power output. The results show that the thermal efficiency of the ORC system with marine diesel exhaust gas as waste heat recovery increases from an average of 35% for conventional engine to 51% and 61% after heat integration. While the performance of conventional types of fuel, such as toluene, benzene, and cyclohexane show thermal efficiency less than 30%.

2. Methodology

In the present research, the selected marine diesel engine consisted of a combination of parameter data from the inline six-cylinder turbocharged engine developed by Hudong Heavy Machinery Co. Ltd., [28] and a dual fuel low-temperature combustion engine [29], which were used as case studies. Table 1 displays the key parameters for the marine diesel engine under design conditions. The exhaust gas heat capacity was used as the air condition, assuming 1.1kJ/kg.K. There were a few assumptions that were applied to the process cycle, where the total mechanical portion of the turbine system and generator might show losses of approximately 5% due to isentropic turbine work; however, the pressure drops were negligible, and the process was in the steady state.

Table 1
 Design condition of parameters for the ORC proposed

Parameters	Symbol	Value	Unit	References
Inlet temperature of exhaust gas	$T_{exh,in} (T_3)$	573.15	K	[28]
Outlet temperature of exhaust gas	$T_{exh,out} (T_4)$	>353.15	K	This study
Mass flow rate of exhaust gas	m_{exh}	9086.61	kg/h	This study
Condensing temperature	T_{cond}	303	K	[29]
Turbine efficiency	η_{turb}	82	%	[29]
Pump efficiency	η_{pump}	80	%	[29]
Inlet temperature of cooling water/seawater	$T_{cw,in}$	298.15	K	[28]
Minimum temperature difference of the condenser	ΔT_{cond}	6.0	K	[28]
Heat exchanger effectiveness	ϵ	0.01	-	[28]
Quality of working fluid leaving evaporator	x	1	-	[28]
Evaporator pressure	P_{evap}	2.0	MPa	[28]
Molecular weight of seawater	$MW_{seawater}$	18.63	kg/kmol	-
Heat capacity of seawater	$Cp_{seawater}$	3.9850	kJ/kg. K	-
Assumption of correction factor for mass flow rate of seawater	α	2	-	This study

The simplest schematic diagram of the ORC system consists of four major component processes, namely, the turbine, condenser, evaporator, and pump. The organic working fluid of the biofuels is heated by exhaust gas from the marine diesel engine in the evaporator (5-5'-6'-6 process), the organic working fluid transforms into vapour and expands in the turbine to create useful work output (6-7 process) before the condensation pressure occurs, and the after-condensed organic working fluid (point 7) is transferred to the condenser (point 7') in order to remove heat until the condensation temperature is reached (7-7'-8'-8 process). The pumping of the organic working fluids must occur when they are condensed in order to reach an absolute liquid state (point 5). In the form of condenser liquid, the organic working fluid is then cooled using seawater. Then, the organic working fluids are pumped from the condenser back to the evaporator (5-6 process). The process of ORC consists of two constant entropy processes, which were at the processes (6-7) and (8-5) where the $dQ=0$, and two constant pressure processes, which were at the process (7-8) and (5-6) where the $dP=0$.

The process of the transformation of working fluids in the ORC component system can be divided into phase changes by sub-transformations by using a thermodynamic analysis based on modelling work. For the complete processes (7-8-5-3) of the marine diesel engine and the ORC system, the cycle of phase would be divided into one-phase after the pump (7-8), two phases in the evaporator (8-5), and the one-phase before the turbine (5-3). After expanding in the turbine to produce the work output at the stream (3-4), a two-phase working fluid after the turbine at the stream (9-4) and a single-phase after condenser at the stream (9-10). Then, the process of the sub-cooler (10-6) occurs for working fluids to condense completely before entering again into the pump to complete the cycle.

In the study, the exhaust gas and seawater outlet temperature in the evaporator and condenser varied with an interval temperature of 5K, while the exhaust gas and seawater inlet temperature remained at constant temperatures of 573.15K, and 298.15K, respectively. The detailed description of an overall ORC system with the parameter data are shown in Figure 1.

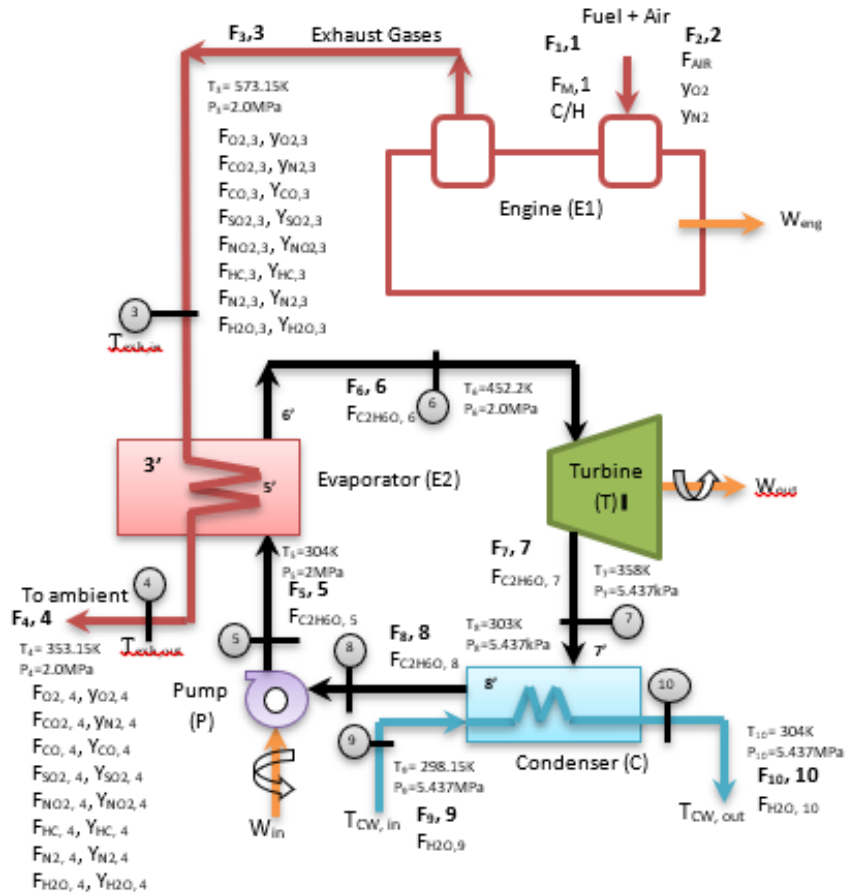
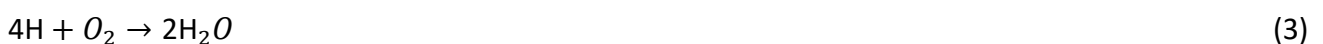


Fig. 1. Flowchart diagram shows the overall ORC system with parameter data

2.1 Material Balance

There are 10 streams involved for the overall material balances in the processing system. The following section explains the development of the material balance equations in each component. The overall combustion reaction involved in a marine diesel engine is given by the following:





The flow rate of the reactant is defined as follows:

$$F_{M,1} = F_{M0} \quad (7)$$

$$F_{AIR} = \left(\frac{F_{N_2} + F_{NO_2}}{y_{N_2}} \right) \quad (8)$$

$$\text{Ratio of HC} = \frac{F_H}{F_C} \quad (9)$$

The product exhaust gas for a marine diesel engine shall be defined as follows:

- The mass balance for oxygen (O₂):

$$F_{O_2} = \frac{(K \times PE)}{MW_{O_2}} \quad (10)$$

- The mass balance for carbon dioxide (CO₂):

$$F_{CO_2} = \frac{(K \times PE)}{MW_{CO_2}} \quad (11)$$

- The mass balance for carbon monoxide (CO):

$$F_{CO} = \frac{(K \times PE)}{MW_{CO}} \quad (12)$$

- The mass balance for sulfur dioxide (SO₂):

$$F_{SO_2} = \frac{(K \times PE)}{MW_{SO_2}} \quad (13)$$

- The mass balance for nitric oxide (NO₂):

$$F_{NO_2} = \frac{(K \times PE)}{MW_{NO_2}} \quad (14)$$

- The mass balance for hydrocarbon (HC):

$$F_{HC} = \frac{(K \times PE)}{MW_{HC}} \quad (15)$$

- The mass balance for nitrogen (N₂):

$$F_{N_2} = \frac{(K \times PE)}{MW_{N_2}} \quad (16)$$

- The mass balance for water (H₂O):

$$F_{H_2O} = \frac{(K \times PE)}{MW_{H_2O}} \quad (17)$$

- The mass balance for C:

$$F_C = \left(\frac{F_{CO_2} \times 1 \text{ mol C}}{1 \text{ mol CO}_2} \right) + \left(\frac{F_{CO} \times 1 \text{ mol C}}{1 \text{ mol CO}} \right) + \left(\frac{F_{HC} \times 1 \text{ mol C}}{1 \text{ mol HC}} \right) \quad (18)$$

- The mass balance for H:

$$F_H = \left(\frac{F_{H_2O} \times 2 \text{ mol H}}{1 \text{ mol H}_2O} \right) + \left(\frac{F_{HC} \times 1 \text{ mol H}}{1 \text{ mol HC}} \right) \quad (19)$$

For a base case of the composition of exhaust gas, in order to determine the fuel used in stream 1, there is need to analyse and solve atomic species balances, which were nH and nC, by using Eq. (18) and Eq. (19). Based on the analysis of the species balance, the results show that the mole amounts of H (nH) and C (nC) are approximately 35.52kmol and 12.52kmol, respectively. Then, the ratio between nH and nC can be calculated using Eq. (9). The fuel composition may therefore be described by the formula $(CH_x)_N$. Since the ratio of H to C is close to 2.84 or approximately 3, the fuel is essentially C_2H_6 and C_3H_8 , perhaps with trace amounts of other hydrocarbons. In this case study, the assumptions regarding the fuel might be derived from C_2H_6 as a burning hydrocarbon. Therefore, the reaction occurring in the marine diesel engine can be found as follows:



The mass balance of the fuel shall be calculated as follows:

- The mass balance for fuel:

$$F_{\text{fuel-C}_2\text{H}_6} = F_{HC} + \left(\frac{F_{CO} \times 1 \text{ mol C}_2\text{H}_6 \text{ consumed}}{2 \text{ mol CO generated}} \right) + \left(\frac{F_{CO_2} \times 1 \text{ mol C}_2\text{H}_6 \text{ consumed}}{2 \text{ mol CO}_2 \text{ generated}} \right) \quad (22)$$

In the ORC system, the mass balance of the cycle is given by the following:

- The mass balance for C_2H_6O :

$$F_{C_2H_6O,5} = F_{C_2H_6O,6} = F_{C_2H_6O,7} = F_{C_2H_6O,8} \quad (23)$$

- The mass balance for H_2O (seawater):

$$F_{H_2O,9} = F_{H_2O,10} \quad (24)$$

2.2 Prediction of Volume Cultivation from Microalgae Culture

The ORC modelling system can be modelled as a closed thermodynamic system which uses four different biofuels, namely, bioethanol, biodiesel, biohydrogen, and biomethane, as organic working fluids from selected microalgae. The selection of microalgae species for bioethanol production was taken from *Chlamydomonas fasciata* Ettl 437, *Dunaliella tertiolecta* and *Synechococcus* PCC 7002,

with yields of approximately 14.4g/L.day, 8-9g/L.day and 30g/L.day, respectively. *Dunaliella salina*, *Nannochloropsis oculata* and *Neochloris oleoabundans* were the species selected for biodiesel production, with lipid productions per day of 116mg/L, 84-142mg/L and 90-134mg/L, respectively. Meanwhile, the yield of *Tetraselmis striata* Butcher from marine green algae was approximately 20.11mL/L, and two species from freshwater green algae, *Chlorella protothecoides* and *Chlorella sp.* with yields of 123.60mL/L and 24mL/L, respectively, were used for biohydrogen production. The selection of microalgae for biomethane was taken from *Dunaliella*, *Chlorella Vulgaris* and *Chlamydomonas reinhardtii*, with yields of approximately 0.44L/g.VS, 0.31-0.35L/g.VS and 0.39L/g.VS, respectively. Any use of methane as a working fluid needs a very low boiling point to be considered, and the pressure in the absorber with correspondingly high system pressures will be large [18]. The biofuels yielded, including bioethanol, biodiesel, biohydrogen, and biomethane, for selected microalgae species are shown in Table 2.

Table 2
 Yield of biofuel production [30-33]

Biofuel	Microalgae	Yield
Bioethanol	<i>Chlamydomonas fasciata</i> Ettl 437	14.4 g/L.day
	<i>Dunaliella tertiolecta</i>	8-9 g/L.day
	<i>Synechococcus</i> PCC 7002	30 g/L.day
Biodiesel	<i>Dunaliella salina</i>	116.0 mg/L/day
	<i>Nannochloropsis oculata</i>	84.0-142.0 mg/L/day
	<i>Neochloris oleoabundans</i>	90.0-134.0 mg/L/day
Biohydrogen	<i>Tetraselmis striata</i> Butcher	20.11 ml/L
	<i>Chlorella protothecoides</i>	123.60 ml/L
	<i>Chlorella sp.</i>	24 ml/L
Biomethane	<i>Dunaliella sp.</i>	0.44 L/g VS
	<i>Chlorella vulgaris sp.</i>	0.31-0.35 L/g VS
	<i>Chlamydomonas reinhardtii sp.</i>	0.39 L/g VS

The volume of cultivation for microalgae was assumed to be approximately 100litres/s. The prediction of the mass flow rate of microalgae can be estimated using Eq. (25), as follows:

$$\dot{m}_{\text{microalgae}} = Y \times V \quad (25)$$

where Y is productivity/ yield of biofuel and V is volume of cultivation.

Therefore, the volume prediction of the microalgae culture for each species can be determined using Eq. (26), as follows:

$$V_{\text{prediction}} = \frac{m_{\text{biofuel}} \times Y}{\dot{m}_{\text{microalgae}}} \quad (26)$$

2.3 Heat Balance

Heat management is a main problem in the ORC system. The system of ORC is the process that will produce electricity with enough heat of transfer. The net output and the ORC system efficiency can be calculated from the energy balance. The ORC system is a conventional process that uses heat to produce work output, which can produce electricity via a generator. The ORC system is developed as a closed type of thermodynamic system. It uses biofuels, such as bioethanol, biodiesel, biohydrogen, and biomethane, from chosen microalgae as an organic working fluid.

2.3.1 Evaporator

The exhaust gas of a marine diesel engine enters the evaporator (E2) at temperature T_3 . Then, from the evaporator, the same composition of exhaust gas will leave the evaporator at temperature T_4 . The exhaust gas transfers heat (Q) to the organic working fluid to reheat the working fluid in the evaporator. Under state 3 to state 4 in the evaporator, the sensible enthalpy of the exhaust gas is used to heat the organic working fluid, which is the used biofuels from state 5 and state 6 in the saturated vapour phase. In the evaporator, the heat loss from the exhaust gas can be determined as follows:

$$Q_{\text{evap, out}} = m_{\text{exh}} C_{p_{\text{exh}}} (T_{\text{exh, in}} - T_{\text{exh, out}}) \quad (27)$$

where the mass flow rate of the exhaust gas in kg/h (m_{exh}), the constant specific heat capacity of the exhaust gas assuming around 1.1kJ/kg.K ($C_{p_{\text{exh}}}$), the outlet temperature of the exhaust gas that leave the evaporator ($T_{\text{exh, out}}$), the inlet temperature of the exhaust gas entering the evaporator ($T_{\text{exh, in}}$), and are lost to the surroundings. Meanwhile, the heat is obtained from the exhaust gas into the organic fluid in the organic fluid streams in the evaporator changing from low to high temperatures before entering the turbine. Therefore, the heat release that can be absorbed from state 5 to 6 in the evaporator is given by the following:

$$Q_{\text{evap, in}} = \frac{m_{\text{wf}}(h_6 - h_5)}{1 - \varepsilon} \quad (28)$$

Eq. (28) for process 5 to 6 can be simplified as follows:

$$Q_{\text{evap, in}} = \frac{m_{\text{wf}} C_{p_{\text{wf}}} (T_6 - T_5)}{1 - \varepsilon} \quad (29)$$

$$\Delta H = \int_{T_3}^{T_4} C_p dT \quad (30)$$

where the heat received from the exhaust gas by the organic fluid (Q_{evap}), the heat exchanger effectiveness (ε) and taken as 0.01 [28], the temperature inlet of the organic working fluid entering the evaporator ($T_{\text{wf, in}}$) and the temperature outlet of the organic working fluid that leaves the evaporator ($T_{\text{wf, out}}$). Enthalpy change and heat received for the working fluid can be calculated using Eq. (29) and (30), respectively, where the $C_{p_{\text{wf}}}$ is heat capacity of biofuels, such as bioethanol (2.100kJ/kg.K), biodiesel (1.850kJ/kg.K), biohydrogen (14.310kJ/kg.K) and biomethane (2.232kJ/kg.K), by assuming that the properties of biofuels are similar to those of conventional substances.

2.3.2 Turbine

The organic working fluid from the evaporator in the superheated vapour phase then enters and expands into the turbine to produce work, where it can cause the generator to produce electricity. The work output at process 6 to 7 in the organic turbine can therefore be calculated and defined as follows:

$$W_{\text{turb, out}} = \eta_{\text{turb}} W_{\text{turb, ideal}} = \eta_{\text{turb}} m_{\text{wf}} (h_6 - h_{7s}) = m_{\text{wf}} (h_6 - h_7) \quad (31)$$

where $W_{\text{turb, out}}$ is known as turbine power for ORC. Therefore, Eq. (31) can be summarized as follows:

$$W_{\text{turb, out}} = \eta_{\text{turb}} m_{\text{wf}} C_{p_{\text{wf}}} (T_{\text{wf, out}} - T_{\text{wf, in}}) \quad (32)$$

where the isentropic efficiency of the turbine at 82% (η_{turb}), the mass flow rate of organic working fluid (m_{wf}) and specific heat capacity of organic working fluid ($C_{p_{\text{wf}}}$), and the outlet and inlet temperatures of the organic working fluid of the turbine for the ideal case ($T_{\text{wf, out}}$ and $T_{\text{wf, in}}$), respectively, and the ideal power of the turbine ($W_{\text{turb, ideal}}$).

2.3.3 Condenser

Afterward, the process proceed with the organic working fluid enters the condenser from the turbine. Then, fluid is converted to the liquid phase from the saturated liquid-vapour mixture phase where it releases heat to the atmosphere from state 7 to state 8 using seawater as the cooling medium. In process 7 to 8, heat rejected in the organic working fluid for the condenser is given by the following:

$$Q_{\text{cond, out}} = \frac{m_{\text{wf}} C_{p_{\text{wf}}} (T_{\text{wf, out}} - T_{\text{wf, in}})}{1 - \varepsilon} \quad (33)$$

where the heat rejected from the organic working fluid to seawater ($Q_{\text{cond, out}}$), the heat exchanger effectiveness (ε), the heat capacity of organic working fluid ($C_{p_{\text{wf}}}$), and the inlet and outlet temperatures of the organic working fluid that enters and leaves the condenser ($T_{\text{wf, in}}$ and $T_{\text{wf, out}}$), respectively.

$$Q_{\text{cond, in}} = \frac{m_{\text{cw}} C_{p_{\text{cw}}} (T_{\text{cw, out}} - T_{\text{cw, in}})}{1 - \varepsilon} \quad (34)$$

However, in the cooling area, $Q_{\text{cond, in}}$ is the heat absorbed by the cooling seawater, ε is the ratio of heat effectiveness of the heat exchanger, $C_{p_{\text{cw}}}$ is the cooling water heat capacity, and $T_{\text{cw, out}}$ and $T_{\text{cw, in}}$ are its outlet and inlet temperatures, respectively.

2.3.4 Pump

Finally, the process proceed with the organic working fluid enters the pump from the condenser in the liquid phase and then is drained and feed to the evaporator unit at such a higher pressure in state 5 to complete the cycle process of ORC. Process 8 to 5 in the organic working fluid pump shall be defined as follows:

$$W_{\text{pump, in}} = \frac{W_{\text{pump, ideal}}}{\eta_{\text{pump}}} = \frac{m_{\text{wf}} (h_5 - h_{8s})}{\eta_{\text{pump}}} = m_{\text{wf}} (h_5 - h_8) \quad (35)$$

where the pump power of the ORC system ($W_{\text{pump, in}}$), the isentropic enthalpy of the organic working fluid after compression in the organic working fluid pump (h_{8s}) and the efficiency of the pump (η_{pump}). However, Eq. (34) can be simplified as follows:

$$W_{\text{pump, in}} = \frac{m_{\text{wf}} C_{p_{\text{wf}}} (T_{\text{wf, out}} - T_{\text{wf, in}})}{\eta_{\text{pump}}} \quad (36)$$

where the ideal power of the pump ($W_{\text{pump, ideal}}$), the isentropic efficiency of the pump for an efficiency of 82% (η_{pump}), the mass flow rate and specific heat capacity of the organic working fluid (m_{wf} and C_{pwf}), respectively, and the outlet and inlet temperatures of the organic working fluid of the pump for the ideal cases ($T_{\text{wf, out}}$ and $T_{\text{wf, in}}$), respectively. The ORC system's net power output can be calculated as below:

$$W_{\text{orc, net}} = W_{\text{turb, out}} - W_{\text{pump, in}} \quad (37)$$

where $W_{\text{orc, net}}$ is the ORC's net power output. The thermal efficiency of the ORC system, η_{net} , can therefore be determined in the following:

$$\eta_{\text{net}} = \frac{W_{\text{orc, net}}}{Q_{\text{evap, out}}} = \frac{W_{\text{turb, out}} - W_{\text{pump, in}}}{Q_{\text{evap, out}}} \quad (38)$$

where $Q_{\text{evap, out}}$ is the heat released from the evaporator.

2.4 Pinch Point and Pinch Point Temperature Difference (PPTD) Analysis

The difference between the exhaust gas temperature and the temperature at which the organic fluid starts to vaporize defined as the pinch point temperature difference (PPTD) [40], in which it plays a significant role in influencing the heat transfer performance. The ORC heat exchanger, which is in the evaporator, this is known as the smallest heat transfer temperature difference and the efficiency limits of the ORC heat exchanger will be determined. The point where the difference in temperature between two fluid streams within the heat exchanger is at a least known as the pinch point, and the difference in temperature at the pinch point known as the PPTD [41]. Jung *et al.*, [41] state that the phase change in the evaporation and condensation processes created an internal pinch point, and PPTD can be identified by plotting the temperatures of the fluids as a function of the heat transfer rate, such as with a T-Q diagram [28]. Analysis of the pinch point temperature in evaporator and condenser can be estimated as follows:

$$T_{\text{pinch, evaporator}} = b(\Delta H_{55'} - \Delta H_{56}) + T_{\text{hs, in}} = \frac{T_{\text{hs, in, 3}} - T_{\text{hs, out, 4}}}{\Delta H_{56}} (\Delta H_{55'} - \Delta H_{56}) + T_3 \quad (39)$$

$$T_{\text{pinch, condenser}} = c(\Delta H_{77'} - \Delta H_{78}) + T_{\text{cw, in}} = \frac{T_{\text{cw, out, 10}} - T_{\text{cw, in, 9}}}{\Delta H_{78}} (\Delta H_{77'} - \Delta H_{78}) + T_9 \quad (40)$$

where b is the slope of line 3-4, and ΔH_{56} and ΔH_{78} are the enthalpy differences between points 5 and 6 and points 7 and 8, respectively. In addition, c is the slope of line 10-9, and $\Delta H_{55'}$ and $\Delta H_{77'}$ are the enthalpy difference between points 5 and 5' and points 7 and 7', respectively. The PPTD for evaporator and condenser can be defined as follows:

$$\text{PPTD}_{\text{evaporator}} = T_{\text{pinch}} - T_{5'} \quad (41)$$

$$\text{PPTD}_{\text{condenser}} = T_{\text{pinch}} - T_{7'} \quad (42)$$

2.5 Heat Integration of the ORC System

Process integration is known as a system-oriented approach to process design in order to sustain overall system development. The use of pinch analysis techniques in heat integration has been recognized as an important tool for analysing and development by process integration of efficient processes [42-45]. The pinch analysis techniques for integrating heat into the ORC component system with a marine diesel engine were used in this paper. As a heat source, the waste heat above the process pinch point was used to integrate with the ORC system for power production. The heat integration in the ORC system with the marine diesel engine achieved the conversion of low-grade energy (waste energy) to high-grade energy through shaft work and electrical power. The result of this application will reduce diesel fuel consumption and enhance system-level energy efficiency as well as energy recovery.

The heat integration in the ORC system never consumes any additional fuel; it is known as an energy-saving measure, and, as a result, reduces the emission of environmental pollutants [44,46]. In the process, there is exhaust gas (hot streams) to be cooled after integrating with organic working fluids (cold streams) to be heated. The modelling of heat integration is focused on evaporator components and two added new components, namely, the superheater and preheater. It is assumed that the superheater and preheater are counter-current heat exchangers with a specified minimum driving force of temperature (ΔT_{\min}). From the sub-cooled liquid phase to the saturated vapour phase, the organic working fluid is heated until superheated vapour is formed (from state 5 to 6). Therefore, in integration, the evaporator is then modelled by adding three sub-units, which are preheating, evaporator (saturated liquid-vapour mixture) and superheating sections. The energy balance is therefore shown as follows for the superheated, two-phase (saturated liquid-vapour mixture), sub-cooled sections and overall evaporator.

$$Q_{\text{evap,sup}} = m_{\text{wf}}m_{\text{wf}}(T_6 - T_{5b}) = m_{\text{exh}}Cp_{\text{exh}}(T_3 - T_{3a}) \quad (43)$$

$$Q_{\text{evap,twp}} = m_{\text{wf}}m_{\text{wf}}(T_{5b} - T_{5a}) = m_{\text{exh}}Cp_{\text{exh}}(T_{3a} - T_{3b}) \quad (44)$$

$$Q_{\text{evap,sub}} = m_{\text{wf}}m_{\text{wf}}(T_{5a} - T_5) = m_{\text{exh}}Cp_{\text{exh}}(T_{3b} - T_4) \quad (45)$$

$$Q_{\text{evap,overall}} = m_{\text{wf}}m_{\text{wf}}(T_6 - T_5) = m_{\text{exh}}Cp_{\text{exh}}(T_3 - T_4) \quad (46)$$

3. Results

3.1 Material Balance

For marine diesel engines, the combined parameters of an inline six-cylinder turbocharged engine manufactured by Hudong Heavy Machinery co., Ltd. and a dual fuel low temperature combustion engine are used. The production of exhaust gas based on the engine output is approximately 996kW by taking the exhaust gas composition content as the main output produced from the main engine [28-29]. The molar flow rate at the stream of (F_3 , 3), for the composition of exhaust gas, can be determined by using Eqs. (10)-(17). The exhaust gas generated from the overall mass balance of a marine diesel engine is determined to contain O_2 : 13.4%, CO_2 : 3.94%, NO_2 : 0.08%, N_2 : 76.99%, and H_2O : 5.59%; also, CO , SO_2 and HC are 0.00% per wet basis, with the total of mass flow rate (F_3 , 3) in wet basis of approximately 9086.61kg/h and that in molar basis of approximately 317.39kmol/h. In the dry basis, the exhaust gas is determined to contain O_2 : 14.19%, CO_2 : 4.17%, NO_2 : 0.08%, and N_2 :

81.55%; also, CO, SO₂ and HC are 0.00%, with the total of mass flow rate (F_3 , 3) in dry basis of approximately 8766.90kg/h and that in molar basis of approximately 299.64kmol/h.

The same gas composition of the exhaust gas is also generated as the only heat transfer to the organic working fluid takes place in the evaporator. Eq. (8), Eq. (18), and Eq. (19) can be used to determine the composition of the exhaust gas, the fuel, and the airflow rate for the base case. In this study, the assumptions regarding the fuels might be derived from C₂H₆ as a hydrocarbon based on the ratio of H to C being close to 3. Based on a determination of the mass balance in the main engine, the fuel (F_1 , 1) was approximately 6.26kmol/h with the air stream supplied, (F_2 , 2) in excess was approximately 309.62kmol/h.

3.2 Pinch Point and Pinch Point Temperature Difference (PPTD)

Eq. (41) and Eq. (42) can be used to calculate the pinch point and PPTD in the evaporator and condenser based on heat output from the evaporator at various biofuel mass flow rates. The pinch point and PPTD increase with the heat absorption increase of the organic working fluids in the evaporator from the research observation. The higher the temperature differential in the evaporator, the lower the heat output from the exhaust gas. Higher heat transfer rates between the exhaust gas and the organic working fluids would therefore be achieved by a suggestion to increase the outlet temperature of exhaust gases. In the meantime, the exhaust gas outlet temperature and the turbine work output have a major effect on the pinch temperature and PPTD for the overall system. However, the PPTD has a positive value. This result shows that the temperature of the pinch was higher than the evaporator's outlet temperature. The outlet temperature of exhaust gas also increases as the PPTD increases, which results in the exhaust heat being completely utilized in the ORC evaporator by showing that the evaporator heat output decreases.

Meanwhile by demonstrating a higher mass flow rate of biofuels, the mass flow rate of biofuels proportionally affects the value of the pinch temperature and PPTD; the pinch temperature and PPTD rose dramatically. The higher the biofuel mass flow rate, the higher the PPTD obtained at the different evaporator heat outputs. The maximum PPTD value showed the highest mass flow rate of biofuels with the lowest exhaust gas heat output, which was approximately 89.51K. In contrast, the lowest mass flow rate of biofuels with heat rejected from the exhaust gas, 610.82kJ/s, showed the smallest PPTD value, which was approximately 5.65K.

The value of PPTD in the condenser is negative. Therefore, in order to show the minimum temperature difference in the condenser as positive, the assumption is made that a negative sign is negligible since it is an interval temperature. As the outlet temperature of seawater increases, the pinch temperature and PPTD also increase. However, in the condenser for seawater, the highest heat available to absorb, the pinch temperature and PPTD are not affected. This outcome might be due to more space being available for heat absorbed in the seawater entering the condenser. From this observation, it is concluded that pinch temperature and PPTD are not sensitive parameters and have an influence when higher heat is absorbed in the cooling water.

However, there is an opposite trend in PPTD when it is affected by the mass flow rate of seawater. The higher the heat rejected in the condenser, the more mass flow rate is needed, and a low PPTD is obtained. The decreasing PPTD will result in efficient heat utilization of the waste heat. In other words, if the PPTD decreases, the evaporating temperature will increase and will result in the area formed by the process of the ORC increasing accordingly. For a given PPTD, a mass flow rate of seawater at a heat rejection of 158.23kJ/s shows a maximal value, while the mass flow rate of seawater at a heat rejection of 107.88kJ/s is minimal; the difference is probably 4kg/s, which is rather high for each biofuel.

3.3 Power Consumption of the Pump

With the rising outlet temperature of the exhaust gas, the power consumption of the pump remains constant for each organic working fluids and shows a trend towards peak power consumption. Wang *et al.*, [45] determined that higher mass flow rates and evaporating pressures will contribute to greater power consumptions.

3.4 Prediction of Volume Cultivation from Microalgae Culture and Cooling Water

For various biofuels, such as bioethanol, biodiesel, biohydrogen, and biomethane, the ORC was analysed at various mass flow rates using specified microalgae. For each biofuel, the mass flow rate ranged from the minimum to the maximum mass flow rate needed for the turbine work output in the 150 to 220kW range. The highest and lowest exhaust gas outlet temperatures of the marine diesel engine were observed in the range of 353.15K to 388.15K with an increment of temperature difference of approximately 5K, where the inlet temperature of exhaust gas is 573.15K with a 9086.61kg/h of mass flow rate. As seen in Figure 2, with the same exhaust gas heat input, the biodiesel mass flow rate is significantly higher than that of the others while biohydrogen has limited flow rate.

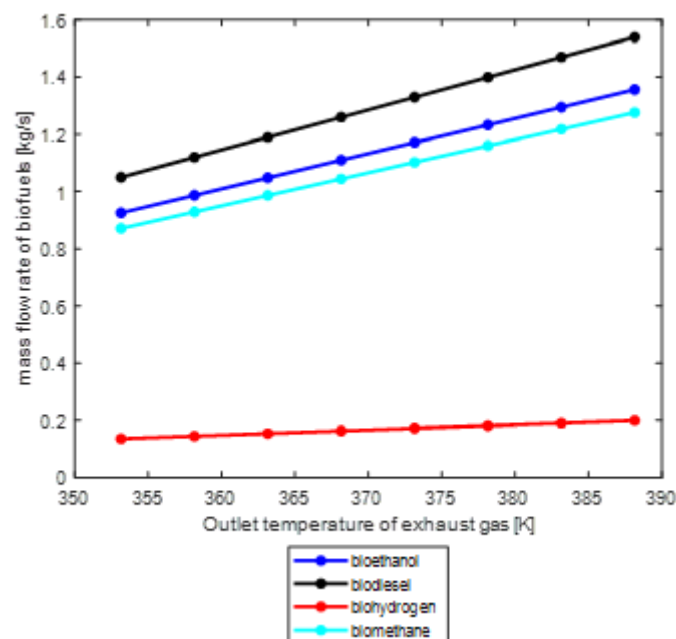


Fig. 2. Mass flow rate of organic Rankine against the outlet temperature of exhaust gas

The mass flow rate of biodiesel is as high as 1.54kg/s, which is 7.7 times that of biohydrogen, which is only 0.2kg/s. Meanwhile, bioethanol and biomethane showed similar behaviour. This outcome is mainly determined by the heat capacity of the biofuels, where the heat capacities of bioethanol, biodiesel, and biomethane are 2.100kJ/kg.K, 1.850kJ/kg.K and 2.232kJ/kg.K, respectively, while biohydrogen is 14.130kJ/kg.K, which is rather higher than bioethanol and the others. Obviously, this trend indicates that the mass flow rate of organic working fluids increases linearly with respect to the exhaust gas's rising outlet temperature. Meanwhile, a certain limit is continually reached by the mass flow rate differential between each organic working fluid.

However, this might be due to the heat available or heat input decreasing linearly and the descent rate of heat capacity of each biofuel varying significantly. Wang *et al.*, [45] state that the descent rate of latent heat of different working fluids might differ greatly.

The organic working fluids in the ORC system used biofuels, such as bioethanol, biodiesel, biohydrogen, and biomethane, from selected microalgae. To determine the amount of mass flow rate needed for use in the ORC system, there was an analysis of time prediction for culturing for microalgae. Table 3 shows the time estimation in days and hours of microalgae cultured from selected species (e.g., bioethanol). There were three species for each biofuels production selected that have been used for analysis. The selection of species was based on a high production yield per day. For bioethanol production, *Chlamydomonas fasciata Ettl 437*, *Dunaliella tertiolecta* and *Synechococcus PCC 7002* were selected, while *Dunaliella salina*, *Nannochloropsis oculata* and *Neochloris oleoabundans* were used for biodiesel production. Meanwhile, for biohydrogen production, *Tetraselmis striata Butcher*, *Chlorella protothecoides* and *Chlorella sp.* were used, while biomethane was produced from species of *Dunaliella*, *Chlorella Vulgaris*, and *Chlamydomonas reinhardtii*. Based on three species of bioethanol, *Synechococcus PCC 7002* showed the faster growth for the production of ethanol compared *Chlamydomonas fasciata Ettl 437* and *Dunaliella tertiolecta*, which needed approximately 0.45 days or 10.85 hours for 13.56g/L. For biodiesel production, *Nannochloropsis oculata* showed the faster growth of approximately 10.84 days or 260.20 hours for 1539.52g/L. *Chlorella protothecoides* showed the shorter times among the three species chosen for culturing, which was approximately 0.023 days or 0.55 hours for biohydrogen production, while biomethane production from *Dunaliella sp.* showed the highest growth for culturing, which was approximately 81.20 days or 1948.86 hours, with a volume expectation of approximately 1.28mg/L.

Table 3
 Times estimation of microalgae culturing for bioethanol from selected species

$m_{\text{bioethanol}}$ (kg/s)	<i>Chlamydomonas fasciata Ettl 437</i>			<i>Dunaliella tertiolecta</i>			<i>Synechococcus PCC 7002</i>		
	Volume prediction, V (g/L)	Culture (days)	Culture (hours)	Volume prediction, V (g/L)	Culture (Days)	Culture (hours)	Volume prediction, V (g/L)	Culture (Days)	Culture (hours)
0.9247	9.25	0.64	14.40	9.25	1.03	24.66	9.25	0.31	7.40
0.9864	9.86	0.68	16.80	9.86	1.10	26.30	9.86	0.33	7.89
1.0480	10.48	0.73	16.80	10.48	1.16	27.95	10.48	0.35	8.38
1.1097	11.10	0.77	19.20	11.10	1.23	29.59	11.10	0.37	8.88
1.1713	11.71	0.81	19.20	11.71	1.30	31.23	11.71	0.39	9.37
1.2330	12.33	0.86	21.60	12.33	1.37	32.88	12.33	0.41	9.86
1.2946	12.95	0.90	21.60	12.95	1.44	34.52	12.95	0.43	10.36
1.3562	13.56	0.94	21.60	13.56	1.51	36.17	13.56	0.45	10.85

This heat was rejected from the organic working fluid in the condenser with the same heat output from organic working fluids and then transformed to the liquid phase where seawater was used in the condenser as cooling water. However, to estimate the mass flow rate of seawater, the heat output from organic working fluids (biofuels) was used as an indicator parameter for the determination. Therefore, by taking the actual seawater mass flow rate as twice the measured mass flow rate, an assumption was made from seawater used in the condenser to determine the actual mass flow rate of seawater. It was to ensure that the liquid phase from the superheated vapour is completely converted. The equation of the actual mass flow rate of seawater as given in Eq. (47):

$$m_{\text{cw,actual}} = 2m_{\text{cw,estimate}} \quad (47)$$

3.5 Heat Integration of ORC System

The proposed model for heat integration of the marine diesel engine and ORC system is applied in this study. In the modelled approach, the system is designed from the perspective of efficient energy utilization through pinch technology. The exhaust gas enters the superheater at T_3 , where the organic working fluids are superheated to a high temperature, T_6 . The exhaust gas then enters the evaporator at T_{3a} , where a mixture of organic working fluids exists in mixed phases (saturated liquid-vapor mixture). The exhaust gas leaves the evaporator at T_{3b} , where T_{3b} is also known as the pinch point temperature, T_{pinch} . The pinch point temperature difference (PPTD) is the temperature difference between T_{3b} and the saturated temperature, T_{sat} . The exhaust gas then enters the preheater at T_{3b} , where the organic working fluids are preheated. The exhaust gas then is discharged to the environment at T_4 with a lower heat loss. However, assumptions were made in the integration analysis, namely, the organic working fluid is in a steady state, a pressure drop on the exhaust gas side does not affect its temperature, with no pressure drops on the organic working fluids side, and the expansion process in the turbine is an isentropic process. It was necessary to shift the temperature where the crossing pinch point between a hot stream and cold stream occurred to make heat transfer in each column successful. The results show that, for temperatures in the range of 353.15K to 363.15K, each biofuel needs to be shifted in temperature in the T-H diagram at the superheater, evaporator, and preheater column after the heat integration. In contrast, for the temperature range of 368.15K to 388.15K, biofuel was not shifted in temperature since they were not in a crossing pinch point in the T-H diagram.

Meanwhile, negative values were determined in the column of the superheater and evaporator for heat available value after the heat integration between a hot stream and cold stream. This negative value was referred to as the heat deficit. However, this deficit value will be balanced when receiving heat in another column; therefore, this will re-balance the heat required in the three columns. As a result, the recovery of exhaust waste heat from the marine diesel engine via the ORC system has been successfully achieved by using this method. Table 4 presents the results for heat recovery and heat losses before and after heat integration at an outlet temperature different from the exhaust gas (e.g., bioethanol). The results show that, after integration, the heat loss was reduced significantly compared to before integration; over 95% of waste heat in the marine diesel engine was recovered after heat integration took place in the power cycle.

Table 4
 Total heat recovery and heat losses of bioethanol before and after heat integration

Outlet temperature of exhaust gas, T_4 (K)	Inlet temperature of biodiesel, T_6 (K)		$W_{turb,out}$ (kW)		W_{net} (kW)	$m_{biofuel}$ (kg/s)	Total energy saving in cold stream (%)		Total heat loss in exhaust gas (%)	
	Before integration	After integration	Before integration	After integration			Before integration	After integration	Before integration	After integration
353.15	452.20	573.15	150	343	340	1.05	47.59	98.75	52.41	1.25
358.15	452.20	567.06	160	355	353	1.12	51.94	97.40	48.06	2.60
363.15	452.20	530.08	170	311	308	1.19	56.50	96.51	43.50	3.49
368.15	452.20	497.20	180	266	263	1.26	61.29	96.13	38.71	3.87
373.15	452.20	467.79	190	221	218	1.33	66.31	96.28	33.69	3.72
378.15	452.20	441.32	200	177	174	1.40	71.59	97.02	28.41	2.98
383.15	452.20	417.36	210	132	129	1.47	77.15	98.38	22.85	1.62
388.15	452.20	395.59	220	88	84	1.54	83.01	100.42	16.99	-0.42

To ensure that the best heat recovery is used in this work with a minimum waste heat loss, a comparison from previous work should be done. Table 5 shows a comparison of heat recovery based on different engine power output with previous work. Based on previous works, marine applications with a power output of 118-258kW can recovery of waste heat loss around 67-82%. Meanwhile, comparing it with this work of power output in range 150-220kW, the highest of heat recovery from the marine engine was around 95-98%. It is expected that working fluid-based biofuels from microalgae via the ORC system have a significant influence in reducing exhaust waste heat from marine diesel engines and recovery it to the system becomes a useful work.

Table 5

Comparison on waste heat recovery of the ORC system based on different engine power output

Parameters	This study						[46]					
Working fluid	bioethanol						R245fa					
Power output (kW)	150	160	170	180	190	200	210	258	236	212	176	118
Waste heat recovery (%)	98	97	95	96	96	97	98	82	81	78	74	67

In this analysis, the condensation temperature of ORC in the condenser column was designed above 300K to reject heat into the surroundings, where a reasonable value of 303K was given. The ambient temperature was assumed as the dead state temperature and kept constant at 298.15K [45]. The evaporating temperature was taken in ranges from the condensing temperature to the heat source temperature. However, the outlet temperature of the heat source is just above the evaporating temperature for heat transfer to occur. All the calculations were developed, and simulations were run using MATLAB. The work output of the turbine before integration initial in the range of 150 to 220kW at different conditions. However, after integration, the turbine's working output increased twice as much as before integration, if the biofuel mass flow rate remained unchanged. It is also suggested that this parameter does not affect the condenser heat rejection and the seawater mass flow rate, even though the flow rate is still unchanged at the turbine work output, the mass flow rate of the biofuels and the specified heat source of the exhaust gas after integration.

3.6 Thermal Efficiency

Figure 3 demonstrates the thermal efficiency of ORC system for each biofuel, namely, bioethanol, biodiesel, biohydrogen and biomethane, before and after heat integration. This figure has shown the thermal efficiency of ORC system in marine diesel engine via biofuel from algae shows the performance at approximately 51% with a net power output of approximately 160kW obtained for each biofuel before integration. After integration, the thermal efficiency improved to 61% with a net power output of approximately 353kW. At this stage, biodiesel presents the highest mass flow rate $1.12\text{kg}\cdot\text{s}^{-1}$ compared to others.

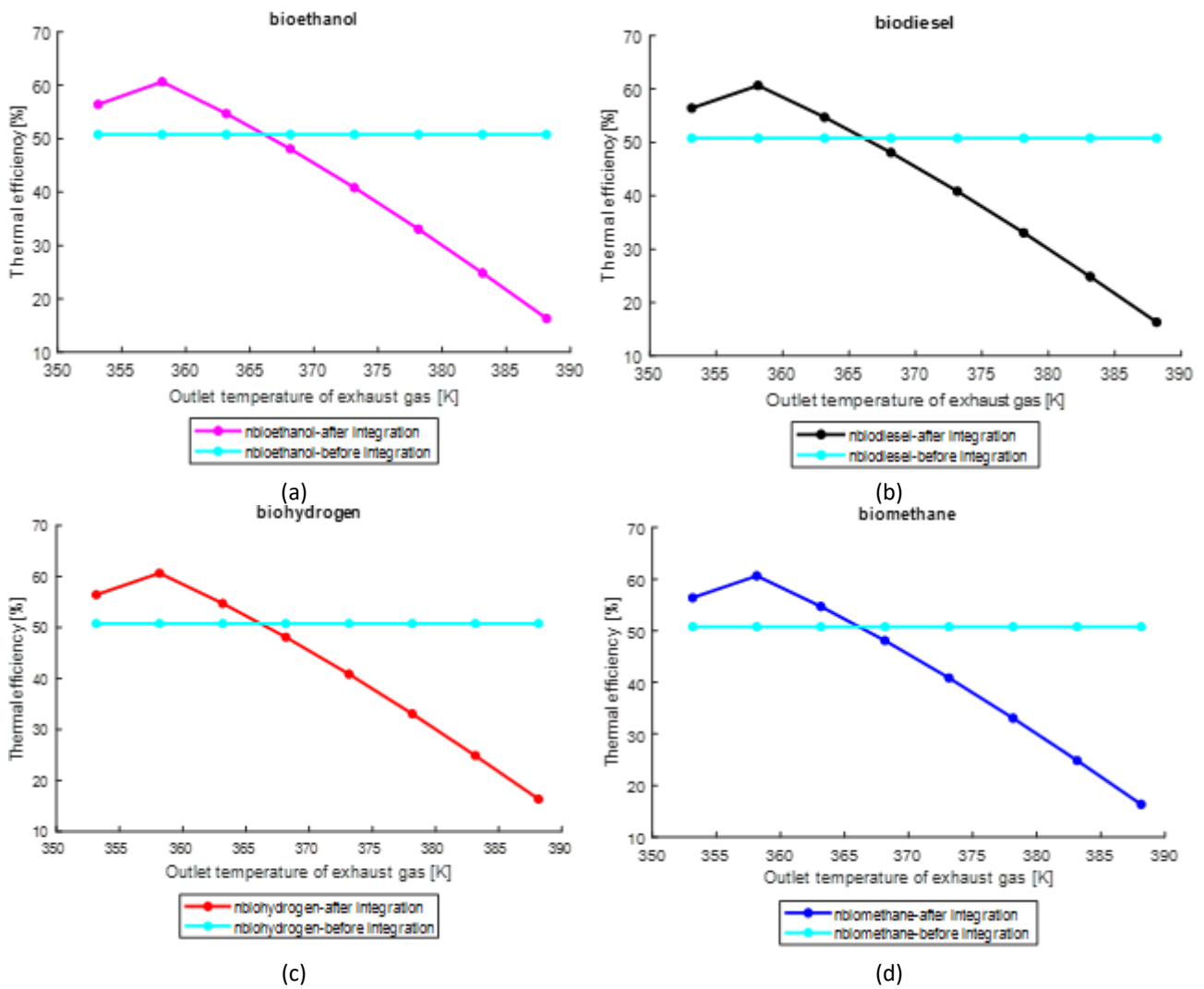


Fig. 3. Variations of thermal efficiency for different biofuel against the outlet temperature of exhaust gas in the ORC system before and after heat integration (a) bioethanol (b) biodiesel (c) biohydrogen (d) biomethane

As the outlet temperature of the exhaust gas increases after integration, the pattern of the figure showing the thermal efficiency for each biofuel increases. In contrast, before integration, thermal efficiency was constant. The trend in thermal efficiency decreased dramatically, however as the outlet temperature of the exhaust gas rose. The decreasing of thermal efficiency was due to the decreasing evaporating temperature. Wang *et al.*, [45] state that the cycle's heat source and heat sink are limited; with an increasing evaporating temperature, a lower heat source temperature will change, resulting in higher thermal efficiency and vice versa. A graph was separately developed for each organic working fluid at this operating exhaust gas temperature to show the trend for each biofuel. In other words, if the higher thermal efficiency is produced, it does not always mean more net power output because it depends on the heat available, where it is always descending [42].

4. Conclusions

The main objective of this research was to study the improvement waste heat recovery and the efficiency of organic Rankine cycle analysis with biofuel from algae for exhaust gas from a marine diesel engine was achieved. This paper expresses the process of the ORC system using different type

of biofuels, namely, bioethanol, biodiesel, biomethane and biohydrogen, from selected microalgae based on the design parameters for each unit. It also shows that the most critical parameters affecting the thermal efficiency of the ORC system are the temperature and the mass flow rate of the exhaust gas. The results obtained are very promising since as working fluid, the biofuel from microalgae has a high potential increase the thermal performance of the ORC system in the marine diesel engine.

Finally, this study predicts the following using microalgae biofuel as a working fluid in the ORC system; first, the ORC system's highest and lowest percentage thermal efficiencies after integration are 61%, and 16% at work of turbine (W_{turb}) are 160kW and 220kW, respectively, compared to the before integration value of approximately 51% at work of turbine (W_{turb}) of 150 to 220kW obtained for each of biofuel. Other studies have found that the ORC system's thermal efficiencies are about 21.0% for toluene, 21.3% for benzene, 21.2% for cyclohexane [28], and 12.7% for R123 [44]. Secondly, after integration, the ORC system's maximum and lowest net power outputs are 353kW and 84kW, respectively, compared to the values before integration of approximately 216kW and 148kW, respectively, for each biofuel. In addition, other studies have shown that the ORC system's net power output was approximately 89.2kW for toluene, 90.8kW for benzene, 90.1kW for cyclohexane [28], and 529kW for R123 [44], respectively. Next, the highest of heat recovery was compared to that before integration, up to almost 95% recovery. Finally, the highest of pump consumptions for each biofuel was approximately 3.56kW.

Acknowledgement

The authors gratefully acknowledge the financial support given for this work by Universiti Kebangsaan Malaysia under PP-SELFUEL-2020.

References

- [1] Nawi, Z. Mat, S. K. Kamarudin, SR Sheikh Abdullah, and S. S. Lam. "The potential of exhaust waste heat recovery (WHR) from marine diesel engines via organic rankine cycle." *Energy* 166 (2019): 17-31. <https://doi.org/10.1016/j.energy.2018.10.064>
- [2] Wu, Binyang, Zhi Jia, Zhen guo Li, Guang yi Liu, and Xiang lin Zhong. "Different exhaust temperature management technologies for heavy-duty diesel engines with regard to thermal efficiency." *Applied Thermal Engineering* 186 (2021): 116495. <https://doi.org/10.1016/j.applthermaleng.2020.116495>
- [3] Thimmanoor, Sai. "Organic Rankine cycle as waste heat recovery system for marine application: Screening methodology, modelling and analysis." (2018).
- [4] Yuan, Xiaolei, Leo Lindroos, Juha Jokisalo, Risto Kosonen, and Yiqun Pan. "Study on waste heat recoveries and energy saving in combined energy system of ice and swimming halls in Finland." *Energy and Buildings* 231 (2021): 110620. <https://doi.org/10.1016/j.enbuild.2020.110620>
- [5] Li, Haoran, Juan Hou, Tianzhen Hong, Yuemin Ding, and Natasa Nord. "Energy, economic, and environmental analysis of integration of thermal energy storage into district heating systems using waste heat from data centres." *Energy* 219 (2021): 119582. <https://doi.org/10.1016/j.energy.2020.119582>
- [6] Bertrand, F. T. "Low-grade heat conversion into power using small scale organic rankine cycles." PhD diss., Doctoral thesis. Agricultural University Of Athens, 2010.
- [7] Hoang, Anh Tuan. "Waste heat recovery from diesel engines based on Organic Rankine Cycle." *Applied energy* 231 (2018): 138-166. <https://doi.org/10.1016/j.apenergy.2018.09.022>
- [8] Ismail, Ainaa Maya Munira, Zurriati Mohd Ali, Kamariah Md Isa, Mohammad Abdullah, and Fazila Mohd Zawawi. "Study On the Potentiality of Power Generation from Exhaust Air Energy Recovery Wind Turbine: A Review." *Journal of Advanced Research in Fluid Mechanics and Thermal Sciences* 87, no. 3 (2021): 148-171. <https://doi.org/10.37934/arfmts.87.3.148171>
- [9] Jung, Hyung-Chul, Susan Krumdieck, and Tony Vranjes. "Feasibility assessment of refinery waste heat-to-power conversion using an organic Rankine cycle." *Energy Conversion and Management* 77 (2014): 396-407. <https://doi.org/10.1016/j.enconman.2013.09.057>
- [10] Al-Janabi, Abdullah, and Nasser Al-Azri. "Effect of recovering the industrial waste heat in Oman on energy and environment." *Energy Reports* 6 (2020): 526-531. <https://doi.org/10.1016/j.egyr.2020.11.203>

- [11] Fekadu, Birlie, and H. V. Harish. "Numerical Studies on Thermo-Hydraulic Characteristics of Turbulent Flow in a Tube with a Regularly Spaced Dimple on Twisted Tape." *CFD Letters* 13, no. 8 (2021): 20-31. <https://doi.org/10.37934/cfdl.13.8.2031>
- [12] Kanungo, Subhrajit, and Tumbanath Samantara. "Numerical Solution of Two-Phase Radiated Unsteady Flow Over a Horizontal Stretching Sheet with Simultaneous Effect of Electrification, Radiation and Non-Uniform Internal Heat Source/Sink." *Journal of Advanced Research in Fluid Mechanics and Thermal Sciences* 100, no. 3 (2022): 11-22. <https://doi.org/10.37934/arfmts.100.3.1122>
- [13] Quoilin, Sylvain, Matthew Orosz, Harold Hemond, and Vincent Lemort. "Performance and design optimization of a low-cost solar organic Rankine cycle for remote power generation." *Solar energy* 85, no. 5 (2011): 955-966. <https://doi.org/10.1016/j.solener.2011.02.010>
- [14] Ibrahim, N., S. Kartom Kamarudin, and L. J. Minggu. "Biofuel from biomass via photo-electrochemical reactions: An overview." *Journal of Power Sources* 259 (2014): 33-42. <https://doi.org/10.1016/j.jpowsour.2014.02.017>
- [15] Yusuf, N. N. A. N., and S. K. Kamarudin. "Techno-economic analysis of biodiesel production from *Jatropha curcas* via a supercritical methanol process." *Energy conversion and management* 75 (2013): 710-717. <https://doi.org/10.1016/j.enconman.2013.08.017>
- [16] Elsayed, Ahmed M. "Design Optimization of Diffuser Augmented Wind Turbine." *CFD Letters* 13, no. 8 (2021): 45-59. <https://doi.org/10.37934/cfdl.13.8.4559>
- [17] Kaushik, Vishal, and Naren Shankar. "Statistical Analysis using Taguchi Method for Designing a Robust Wind Turbine." *Journal of Advanced Research in Fluid Mechanics and Thermal Sciences* 100, no. 3 (2022): 92-105. <https://doi.org/10.37934/arfmts.100.3.92105>
- [18] Shamsul, N. S., S. K. Kamarudin, and N. A. Rahman. "Conversion of bio-oil to bio gasoline via pyrolysis and hydrothermal: A review." *Renewable and Sustainable Energy Reviews* 80 (2017): 538-549. <https://doi.org/10.1016/j.rser.2017.05.245>
- [19] Vijayaraghavan, Sanjay, and D. Yogi Goswami. "On evaluating efficiency of a combined power and cooling cycle." *J. Energy Resour. Technol.* 125, no. 3 (2003): 221-227. <https://doi.org/10.1115/1.1595110>
- [20] Wang, Hui-Yuan, David Bluck, and Bernard J. Van Wie. "Conversion of microalgae to jet fuel: Process design and simulation." *Bioresource technology* 167 (2014): 349-357. <https://doi.org/10.1016/j.biortech.2014.05.092>
- [21] Hossain, ABM Sharif, Aishah Salleh, Amru Nasrulhaq Boyce, Partha Chowdhury, and Mohd Naquiuddin. "Biodiesel fuel production from algae as renewable energy." *American journal of biochemistry and biotechnology* 4, no. 3 (2008): 250-254. <https://doi.org/10.3844/ajbb.2008.250.254>
- [22] Amaro, Helena M., Ângela C. Macedo, and F. Xavier Malcata. "Microalgae: an alternative as sustainable source of biofuels?." *Energy* 44, no. 1 (2012): 158-166. <https://doi.org/10.1016/j.energy.2012.05.006>
- [23] Ziolkowska, Jadwiga R., and Leo Simon. "Recent developments and prospects for algae-based fuels in the US." *Renewable and Sustainable Energy Reviews* 29 (2014): 847-853. <https://doi.org/10.1016/j.rser.2013.09.021>
- [24] Harun, Razif, Manjinder Singh, Gareth M. Forde, and Michael K. Danquah. "Bioprocess engineering of microalgae to produce a variety of consumer products." *Renewable and sustainable energy reviews* 14, no. 3 (2010): 1037-1047. <https://doi.org/10.1016/j.rser.2009.11.004>
- [25] Lang, Kwong Cheng, Lian See Tan, Jully Tan, Azmi Mohd Shariff, and Hairul Nazirah Abdul Halim. "Life cycle assessment of potassium lysinate for biogas upgrading." *Progress in Energy and Environment* 22 (2022): 29-39. <https://doi.org/10.37934/progee.22.1.2939>
- [26] Schenk, Peer M., Skye R. Thomas-Hall, Evan Stephens, Ute C. Marx, Jan H. Mussnug, Clemens Posten, Olaf Kruse, and Ben Hankamer. "Second generation biofuels: high-efficiency microalgae for biodiesel production." *Bioenergy research* 1 (2008): 20-43. <https://doi.org/10.1007/s12155-008-9008-8>
- [27] Nima, Nayema Islam, and Mohammad Ferdows. "Dual Solutions in Mixed Convection Flow Along Non-Isothermal Inclined Cylinder Containing Gyrotactic Microorganism." *Journal of Advanced Research in Fluid Mechanics and Thermal Sciences* 87, no. 3 (2021): 51-63. <https://doi.org/10.37934/arfmts.87.3.5163>
- [28] Song, Jian, Yin Song, and Chun-wei Gu. "Thermodynamic analysis and performance optimization of an Organic Rankine Cycle (ORC) waste heat recovery system for marine diesel engines." *Energy* 82 (2015): 976-985. <https://doi.org/10.1016/j.energy.2015.01.108>
- [29] Srinivasan, Kalyan K., Pedro J. Mago, and Sundar R. Krishnan. "Analysis of exhaust waste heat recovery from a dual fuel low temperature combustion engine using an Organic Rankine Cycle." *Energy* 35, no. 6 (2010): 2387-2399. <https://doi.org/10.1016/j.energy.2010.02.018>
- [30] Song, Jian, Yan Li, Chun-wei Gu, and Li Zhang. "Thermodynamic analysis and performance optimization of an ORC (Organic Rankine Cycle) system for multi-strand waste heat sources in petroleum refining industry." *Energy* 71 (2014): 673-680. <https://doi.org/10.1016/j.energy.2014.05.014>

- [31] de Farias Silva, Carlos Eduardo, and Alberto Bertucco. "Bioethanol from microalgae and cyanobacteria: a review and technological outlook." *Process Biochemistry* 51, no. 11 (2016): 1833-1842. <https://doi.org/10.1016/j.procbio.2016.02.016>
- [32] Mata, Teresa M., Antonio A. Martins, and Nidia S. Caetano. "Microalgae for biodiesel production and other applications: a review." *Renewable and sustainable energy reviews* 14, no. 1 (2010): 217-232. <https://doi.org/10.1016/j.rser.2009.07.020>
- [33] He, Meilin, Ling Li, and Jianguo Liu. "Isolation of wild microalgae from natural water bodies for high hydrogen producing strains." *international journal of hydrogen energy* 37, no. 5 (2012): 4046-4056. <https://doi.org/10.1016/j.ijhydene.2011.11.089>
- [34] González-Fernández, Cristina, Bruno Sialve, Nicolas Bernet, and Jean-Philippe Steyer. "Impact of microalgae characteristics on their conversion to biofuel. Part II: Focus on biomethane production." *Biofuels, Bioproducts and Biorefining* 6, no. 2 (2012): 205-218. <https://doi.org/10.1002/bbb.337>
- [35] Rakopoulos, C. D., K. A. Antonopoulos, and D. C. Rakopoulos. "Experimental heat release analysis and emissions of a HSDI diesel engine fueled with ethanol–diesel fuel blends." *Energy* 32, no. 10 (2007): 1791-1808. <https://doi.org/10.1016/j.energy.2007.03.005>
- [36] Yusuf, N. N. A. N., S. K. Kamarudin, and Z. Yaakub. "Overview on the Current URL: <https://www.trijurnal.lmlit.trisakti.ac.id/index.php/jeeset>, DOI: <https://dx.doi.org/10.25105/jeeset.v5i2.12756> Trends in Biodiesel Production." *Energy Conversion and Management* 52, no. 7 (2011): 2741-2751. <https://doi.org/10.1016/j.enconman.2010.12.004>
- [37] Demirbas, Ayhan. "Progress and recent trends in biofuels." *Progress in energy and combustion science* 33, no. 1 (2007): 1-18. <https://doi.org/10.1016/j.peccs.2006.06.001>
- [38] Freitas, Samuel VD, Mariana B. Oliveira, Álvaro S. Lima, and João AP Coutinho. "Measurement and prediction of biodiesel volatility." *Energy & fuels* 26, no. 5 (2012): 3048-3053. <https://doi.org/10.1021/ef3004174>
- [39] Cunico, Larissa P., Roberta Ceriani, and Reginaldo Guirardello. "Estimation of physical properties of vegetable oils and biodiesel using group contribution methods." *CHEMICAL ENGINEERING* 32 (2013).
- [40] Saxena, Parag, Sayali Jawale, and Milind H. Joshipura. "A review on prediction of properties of biodiesel and blends of biodiesel." *Procedia engineering* 51 (2013): 395-402. <https://doi.org/10.1016/j.proeng.2013.01.055>
- [41] El-Wakil, Mohamed Mohamed. "Powerplant technology." (1984).
- [42] Cherubini, Francesco. "The biorefinery concept: using biomass instead of oil for producing energy and chemicals." *Energy conversion and management* 51, no. 7 (2010): 1412-1421. <https://doi.org/10.1016/j.enconman.2013.09.057>
- [43] Kemp, Ian C. *Pinch analysis and process integration: a user guide on process integration for the efficient use of energy*. Elsevier, 2011.
- [44] Linnhoff, Bodo. "Pinch technology for the synthesis of optimal heat and power systems." (1989): 137-147. <https://doi.org/10.1115/1.3231415>
- [45] Wang, Dongxiang, Xiang Ling, and Hao Peng. "Performance analysis of double organic Rankine cycle for discontinuous low temperature waste heat recovery." *Applied Thermal Engineering* 48 (2012): 63-71. <https://doi.org/10.1016/j.applthermaleng.2012.04.017>
- [46] Yu, Guopeng, Gequn Shu, Hua Tian, Haiqiao Wei, and Lina Liu. "Simulation and thermodynamic analysis of a bottoming Organic Rankine Cycle (ORC) of diesel engine (DE)." *Energy* 51 (2013): 281-290. <https://doi.org/10.1016/j.energy.2012.10.054>
- [47] Abidin, Nurul Hafizah Zainal, Nor Fadzillah Mohd Mokhtar, Izzati Khalidah Khalid, and Siti Nur Aisyah Azeman. "Oscillatory Mode of Darcy-Rayleigh Convection in a Viscoelastic Double Diffusive Binary Fluid Layer Saturated Anisotropic Porous Layer." *Journal of Advanced Research in Numerical Heat Transfer* 10, no. 1 (2022): 8-19.